Thermal stability of patterned Co/Pd nanodot arrays

I. Tudosa,[a] Marko V. Lubarda, K. T. Chan, M. A. Escobar, Vitaliy Lomakin, and E. E. Fullerton[b]
Center for Magnetic Recording Research, University of California, San Diego, La Jolla, California 92093-0401, USA

(Received 17 December 2011; accepted 3 February 2012; published online 5 March 2012)

We have studied the magnetic reversal and thermal stability of $[Co(0.3\,nm)/Pd(0.7\,nm)]_N$ multilayers patterned into 35-nm-diameter nanodot arrays. The short-time coercive fields are relatively constant with N while the room-temperature thermal stability parameter increases nearly linearly with N. However the magnetic switching volume extracted from the thermal stability is significantly less than the physical volume of the samples. The experimental results are in quantitative agreement with micromagnetic modeling, which indicates that reversal and thermal stability is controlled by nucleation and propagation of edge domains. © *2012 American Institute of Physics*. [http://dx.doi.org/10.1063/1.3692574]

Patterned magnetic structures obtained either by self-organization or standard lithography enjoy intense research activity.[1] This interest is driven partly not only by emergent physics as films are laterally confined but also by the potential of nanomagnetism-based materials in applications such as high-density magnetic data storage,[2] magnetic memory,[3,4] logic devices,[5] and biomedical applications.[6] One example is bit patterned media (BPM) which is a leading candidate to extend magnetic recording to densities beyond those achievable by perpendicular magnetic recording on continuous granular media.[2,7,8] In BPM the bits are lithographically predefined as islands so that the magnetic volume relevant for thermal stability is the entire bit volume rather than the much smaller volumes of the individual grains that form the bit in continuous recording.

In the recent literature there has been considerable focus on the control and understanding of the switching field and switching field distributions of patterned islands.[9–15] In contrast, there have been relatively few published results on the thermal stability of BPM (Ref. 14) and related perpendicular anisotropy devices[16] even though stability is the major motivation for the implementation of BPM. In this letter we describe an experimental and theoretical study of the thermal stability of patterned arrays fabricated from Co/Pd multilayer films. We find that for 35-nm diameter islands that the magnetic switching volume extracted from the thermal stability is significantly less than the physical volume of the samples. The experimental results are in quantitative agreement with micromagnetic modeling which indicated that reversal and thermal stability is controlled by nucleation and propagation of edge domains.

The starting continuous multilayer films were Ta(3 nm)/Pd(3 nm)/$[Co(0.3\,nm)/Pd(0.7\,nm)]_N$/Cr(0.2 nm) films on SiOx coated Si wafers where the number of repeat $N = 3$, 5, 8, or 11. These films were grown by DC magnetron sputtering and have strong perpendicular anisotropy with an anisotropy field H_K of 21 kOe estimated from saturation field of the hard axis loops. This H_K value is the effective anisotropy that includes both the shape and magneto-crystalline anisotropies. The nanodot arrays were fabricated by Ar ion milling and the continuous magnetic films using self-assembling polymer [polystyrene–poly(methyl methacrylate) (PS–PMMA)] annealed at 200 °C as the patterning mask. The PMMA dots are selectively removed by oxygen plasma etching and the resulting holes were filled with spin-on-glass (SOG) that acts as the etch mask as described in Refs. 8 and 17. The underlying magnetic films were patterned by Ar ion milling through the SOG mask. The resulting island size was 35-40 nm with a 65-nm pitch over macroscopic areas. Electron microscopy images are shown in Figs. 1(a) and 1(b).

We used magneto-optic Kerr effect (MOKE) and vibrating sample magnetometry to characterize the magnetic properties. As typically seen, there is a large increase in the coercivity (H_C) with patterning and a broadening of the hysteresis loop that reflects the switching field distribution (SFD) of the islands.[9,12] The coercive fields are given in Table I. To extract the total SFD and intrinsic contributions to the SFD, we used the ΔH(M, ΔM) method that analyzes a sequence of minor loops.[12] Given in Table I are the total and intrinsic SFD (without the interaction contributions) given by σ_{tot} and σ_{int}, respectively.

Thermal stability parameters of the films were extracted from the field sweep rate dependence of the coercive fields shown in Fig. 1(c). This data was fit using

$$H_c = H_0\left[1 - \left(\frac{1}{a}\ln\left(\frac{f_0 H_0}{2a}\frac{1}{R}\right)\right)^n\right], \quad (1)$$

where f_0 is the attempt frequency of about 10^{10} Hz, the exponent $n = 2/3$ is used, R is the magnetic field sweep rate which varied over three orders of magnitude, H_0 is the field at which the activation energy vanishes and $a = K_u V/k_B T$ is the ratio of anisotropy barrier to thermal energy. The results for $K_u V$ and H_0 are given in Table I. The results are relatively insensitive to the parameters chosen in Eq. (1). Using $n = 1/2$ gives roughly a 20% difference in fitted parameters and

[a]Current address: SLAC National Accelerator Laboratory, 2575 Sand Hill Rd, MSC 19, Menlo Park, California 94025, USA.
[b]Author to whom correspondence should be addressed. Electronic mail: efullerton@ucsd.edu.

 © 2012 American Institute of Physics

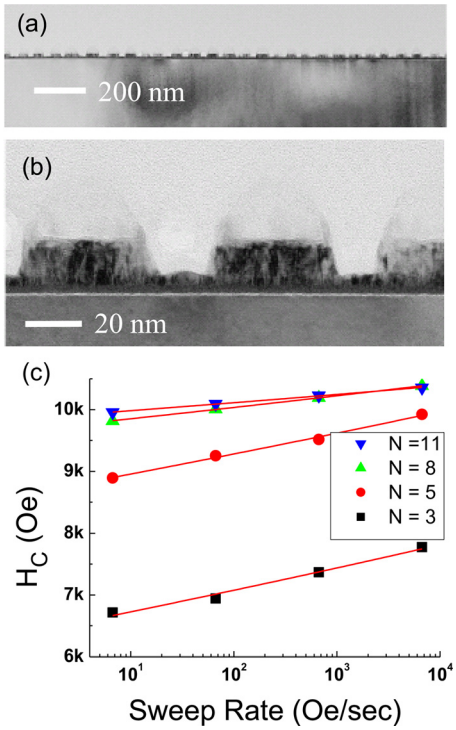

FIG. 1. (Color online) Lower (a) and higher (b) resolution images of patterned $[Co(0.3\,nm)/Pd(0.7\,nm)]_{11}$ multilayers. (c) Time-dependent coercive fields for N = 3, 5, 8, and 11. The solid lines are fits to Eq. (1) with the fit parameters given in Table I.

increasing and decreasing f_0 by an order of magnitude results in <5% change in the stability parameter.

Before discussing the stability results in detail we discuss the results in Table I. The H_0 values are relatively insensitive to N and are centered about 12.5 kOe, roughly 60% of the anisotropy field. The thermal stability parameter increases systematically with N from $80k_BT$ for $N=3$ to $360k_BT$ for $N=11$. Consistent with increasing energy barrier the difference between H_C and H_0 decreases with increasing N. For all N we find $\sigma_{tot} > \sigma_{int}$ indicating that the interaction between islands are antiferromagnetic in nature consistent with dipolar interactions being the dominate interaction. The difference $\sigma_{tot} - \sigma_{int}$ gives the mean dipolar interaction which increases systematically from 35 Oe for $N=3$ to 235 Oe for $N=11$ that reflects the increased moment of the adjacent islands with increasing N. The measured σ_{tot} are ~8% of H_0, independent of N consistent with published literature for patterned Co/Pd multilayers of similar size.[12]

TABLE I. Magnetic properties of patterned $[Co(0.3\,nm)/Pd(0.7\,nm)]_N$ multilayers for various N. K_UV/k_BT and H_0 were determined form time dependent coercive fields (Fig. 1(c)) according to Eq. (1). The total and intrinsic SFDs, σ_{tot} and σ_{int}, respectively, were determined from minor loop analysis.

	$N=3$	$N=5$	$N=9$	$N=11$
H_C (kOe)	7.6	9.7	10.4	10.3
H_0 (kOe)	12.3	14.2	12.6	11.9
σ_{tot} (Oe)	1058	1127	1214	1191
σ_{int} (Oe)	1023	1040	1026	936
σ_{int}/H_0	8.3%	7.3%	8.1%	7.9%
K_UV/k_BT	80	110	230	360

As stated earlier, the island stability increases with increasing N which would be expected as the volume of the island increased and, based on the coercivity results, the anisotropy is insensitive to N. However a simple calculation of the expected energy barrier assuming a macrospin reversal gives values much higher than the measured barriers. Using the measured H_0 as an estimate of the anisotropy field ($H_0 = 2K_U/M_S = 12$ kOe) and the volume averaged magnetization ($M_S = 700\,emu/cm^3$) gives $K_U = 4.2 \times 10^6$ ergs/cm^3. The estimated volume is $V = 2.9 \times 10^3$ nm^3 for the $N=3$ islands yielding an expected room-temperature $K_UV/k_BT = 290$ roughly a factor of 3.7 larger than what we measure. If we assume the anisotropy is the unpatterned thin filmed value of 21 kOe the difference between the measured and expected stability is even larger. This trend holds for all the islands studied. In general, lower energy barriers suggest that the islands reverse via a non-coherent mode. Since the measured barrier increases linearly with N, the mode most likely involves a lateral domain wall in the island as opposed to a vertical domain wall enabled by the relatively weak exchange coupling across the Pd layer.[18]

To gain further insight into the magnetization reversal we compared the experimental results to micromagnetic simulations obtained using the FastMag simulator, which rapidly and accurately solves the Landau-Lifshitz-Gilbert equation with discretization chosen to obtain full convergence.[19] For the energy barrier we calculated both the macrospin barrier including the appropriate shape anisotropy as well as the minimum energy barrier using an extension of FastMag (Refs. 19 and 20), which implement the nudge elastic band (NEB) method accounting for non-uniform magnetization along the minimum path. The micromagnetic parameters were chosen to match the properties of the Co/Pd multilayers[18] and the anisotropy was adjusted to match the measured short-time coercive field. An example calculation of the minimum energy path for an $N=5$ island is shown in Fig. 2(a). Reversal in zero applied magnetic field occurs by nucleation of an edge domain and propagation of a domain wall. The energy barrier height is set by the energy of a domain wall in the center of the island. This energy of 130 k_BT is significantly less than the macrospin value 440 k_BT.

Plotted in Fig. 2(b) are the measured energy barriers, the micromagnetically calculated macrospin and minimum energy barrier vs. N. The micromagnetic barrier is calculated in the high-coupling limit, assuming relatively strong exchange across the Pd layers such that the Co layers do not reverse individually. There is close agreement between the micromagnetically calculated and measured energy barriers dependence on N and that the barrier values are significantly smaller than the macrospin expectations. For the range of N studied, the calculated barriers are relatively insensitive to the interlayer exchange coupling for the range studied. For relatively low interlayer exchange coupled islands begin to reverse via a vertical domain wall that nucleates at the surface of the island.[18] Once the island becomes thicker than the vertical domain wall, the energy barrier becomes independent of thickness and is set by the domain wall energy. For even lower exchange, reversal can occurs by individual Co layers as will be discussed elsewhere.

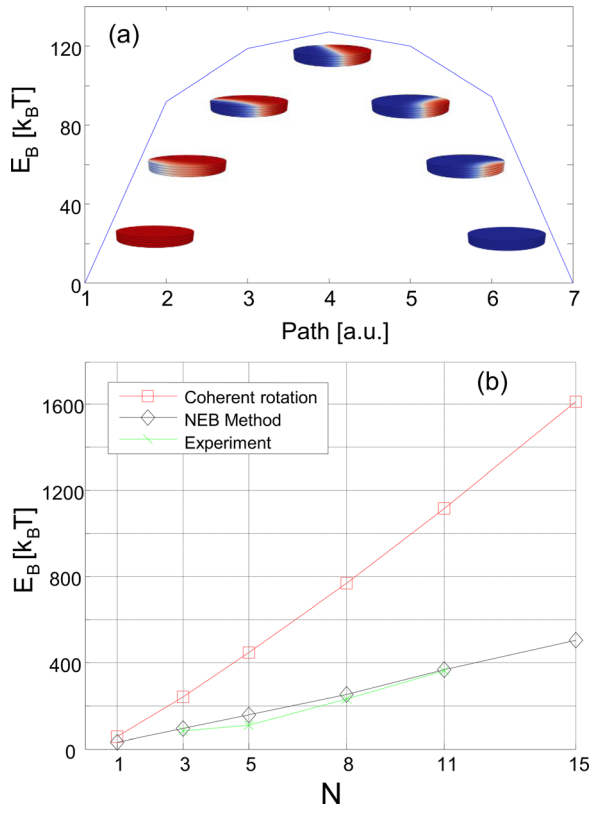

FIG. 2. (Color online) (a) Micromagnetic results for the minimum energy reversal pathway for a 35-nm diameter $[Co(0.3\,nm)/Pd(0.7\,nm)]_5$ multilayer. Domain images are shown along the path indicating a reversal mode consisting of edge domain nucleation and lateral propagation. The energy is maximum when the domain wall extends across the full diameter of the island. (b) Micromagnetic (black diamonds and red squares) and experimental (green crosses) results for the energy barrier vs. *N*. The micromagnetic calculations include the minimum energy reversal pathway NEB results assuming the strong coupling limit (black diamonds) and the macrospin result assuming coherent rotation (red squares) including the appropriate shape anisotropy and the minimum energy barrier.

These results give reasonable confidence that for 35-nm diameter, the energy barrier is determined by nucleation of edge domains that reverse the island by domain wall motion. This is consistent with recent measurements of perpendicular anisotropy spin-torque devices where the measured energy barrier for a 50×100 nm^2 nanopillar was a factor of 6 lower than the macrospin estimates.[16] Also, spin-torque induced domain states have been observed in similar pillars.[21,22] Previous measurement and modeling of patterned Co/Pd multilayers for different island size suggested that both the coercivity and the SFDs versus island size could be understood assuming that reversal was controlled by regions on the order of 20 nm.[9] These results are consistent with the current findings and reverse domains seen in Fig. 2(a).

Fig. 3 shows the calculated energy barriers as a function of island diameter ranging from 40 to 5 nm compared to the macrospin energy. The difference between the macrospin and minimum energy barrier persists down to ~10-nm diameters. Even at 20-nm island size there is a factor of 2 reduction of the energy barrier compared to the macrospin. For applications such as patterned media, the issue of reduced energy barriers due to incoherent reversal will most likely not be an issue. The expected island sizes will be 12.5 nm at 1 Tb/in^2 densities where the macrospin approximation is

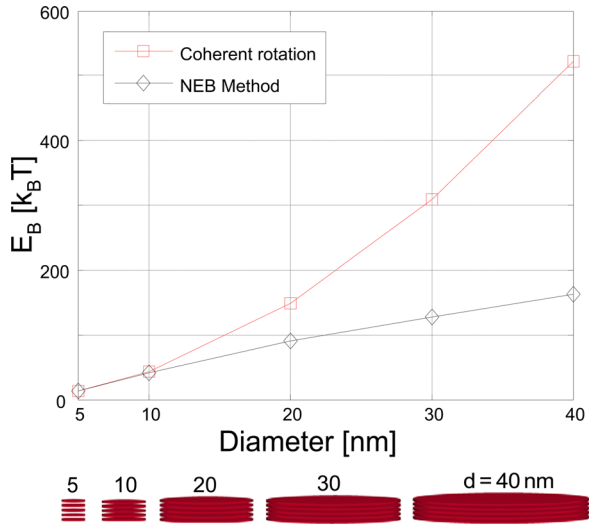

FIG. 3. (Color online) Micromagnetic results for the minimum energy reversal pathway (NEB results) for $[Co(0.3\,nm)/Pd(0.7\,nm)]_5$ multilayer islands ranging from 5 nm to 40 nm in diameter compared to the macrospin approximation.

valid. For applications such as spin-transfer-torque (STT) magnetic random access memories (MRAM), incoherent reversal may be more important. Perpendicular anisotropy devices are anticipated for high-density STT-MRAM.[23,24] The critical current scales are expected to scale with the macrospin energy barrier, and device sizes are anticipated to be similar to those discussed here. However, the energy barrier will need to be calculated for the particular material set and will depend on the specifics of the magnetization density, anisotropy, and domain wall energies and size.

In conclusion, we have studied the magnetic reversal of patterned Co/Pd multilayers as a function of the number of Co/Pd layers and island diameter in the high coupling limit. Experimental results revealed a significant discrepancy between the extracted thermal stability of the islands and thermal stability estimates based on the macrospin model, implying an incoherent mode of reversal. Micromagnetic results were in close quantitative agreement with experimental measurements, and showed that thermal reversal begins by nucleation of an edge domain, followed by lateral domain wall propagation. These results show that incoherent reversal modes in islands as small as a few tens of nanometers in diameter can play a significant role in determining the thermal stability of the structure and reliability of information storage.

We would like to acknowledge financial support from INSIC through the EDHR program and collaborations with Toshiba Research on the patterning of the samples.

[1]J. I. Martin, J. Nogues, K. Liu, J. L. Vicent, and I. K. Schuller, J. Magn. Magn. Mater. **256**, 449 (2003).
[2]B. D. Terris and T. Thomson, J. Phys. D **38**, R199 (2005).
[3]B. N. Engel, J. Akerman, B. Butcher, R. W. Dave, M. DeHerrera, M. Durlam, G. Grynkewich, J. Janesky, S. V. Pietambaram, N. D. Rizzo, J. M. Slaughter, K. Smith, J. J. Sun, and S. Tehrani, IEEE Trans. Mag. **41**, 132 (2005).
[4]W. J. Gallagher and S. S. P. Parkin, IBM J. Res. Dev. **50**, 5 (2006).
[5]Dery, P. Dalal, L. Cywinski, and L. J. Sham, Nature **447**, 573 (2007).
[6]D. A. Hall, R. S. Gaster, T. Lin, S. J. Osterfeld, S. Han, B. Murmann, and S. X. Wang, Biosens. Bioelectron. **25**, 2051 (2010).

[7]A. Moser, K. Takano, D. T. Margulies, M. Albrecht, Y. Sonobe, Y. Ikeda, S. H. Sun, and E. E. Fullerton, J. of Phys. D-Appl. Phys. **35**, R157 (2002).
[8]A. Kikitsu, Y. Kamata, M. Sakurai, and K. Naito, IEEE Trans. Magn. **43**, 3685 (2007).
[9]T. Thomson, G. Hu, and B. D. Terris, Phys. Rev. Lett. **96**, 257204 (2006).
[10]H. J. Richter, A. Y. Dobin, R. T. Lynch, D. Weller, R. M. Brockie, O. Heinonen, K. Z. Gao, J. Xue, R. J. M. Veerdonk, P. Asselin, and M. F. Erden, Appl. Phys. Lett. **88**, 222512 (2006).
[11]P. Krone, D. Makarov, T. Schrefl, and M. Albrecht, J. Appl. Phys. **106**, 103913 (2009).
[12]O. Hellwig, A. Berger, T. Thomson, E. Dobisz, Z. Bandic, H. Yang, D. S. Kercher, and E. E. Fullerton, Appl. Phys. Lett. **90**, 162516 (2007).
[13]O. Hellwig, T. Hauet, T. Thomson, E. Dobisz, J. D. Risner-Jamtgaard, D. Yaney, B. D. Terris, and E. E. Fullerton, Appl. Phys. Lett. **95**, 232505 (2009).
[14]J. M. Shaw, S. E. Russek, T. Thomson, M. J. Donahue, B. D. Terris, O. Hellwig, E. Dobisz, and M. L. Schneider, Phys. Rev. B **78**, 024414 (2008).
[15]J. M. Shaw, H. T. Nembach, T. J. Silva, S. E. Russek, R. Geiss, C. Jones, N. Clark, T. Leo, and D. J. Smith, Phys. Rev. B **80**, 184419 (2009).
[16]D. Bedau, H. Liu, J. Z. Sun, J. A. Katine, E. E. Fullerton, S. Mangin, and A. D. Kent, Appl. Phys. Lett. **97**, 262502 (2010).
[17]Y. Kamata, A. Kikitsu, H. Hieda, M. Sakurai, and K. Naito, J. Appl. Phys. **95**, 6705 (2004).
[18]S. M. Watson, T. Hauet, J. A. Borchers, S. Mangin, and E. E. Fullerton, Appl. Phys. Lett. **92**, 202507 (2008).
[19]R. Chang, S. Li, M. V. Lubarda, B. Livshitz, and V. Lomakin, J. Appl. Phys. **110**, 039907 (2011).
[20]R. Dittrich, T. Schrefl, D. Suess, W. Scholz, H. Forster, and J. Fidler, J. Magn. Magn. Mater. **250**, L12 (2002).
[21]D. Ravelosona, S. Mangin, Y. Lemaho, J. A. Katine, B. D. Terris, and E. E. Fullerton, Phys. Rev. Lett. **96**, 186604 (2006).
[22]J. Cucchiara, Y. Henry, D. Ravelosona, D. Lacour, E. E. Fullerton, J. A. Katine, and S. Mangin, Appl. Phys. Lett. **94**, 102503 (2009).
[23]S. Mangin, Y. Henry, D. Ravelosona, J. A. Katine, and E. E. Fullerton, Appl. Phys. Lett. **94**, 012502 (2009).
[24]S. Ikeda, K. Miura, H. Yamamoto, K. Mizunuma, H. D. Gan, M. Endo, S. Kanai, J. Hayakawa, F. Matsukura, and H. Ohno, Nat. Mater. **9**, 721 (2010).